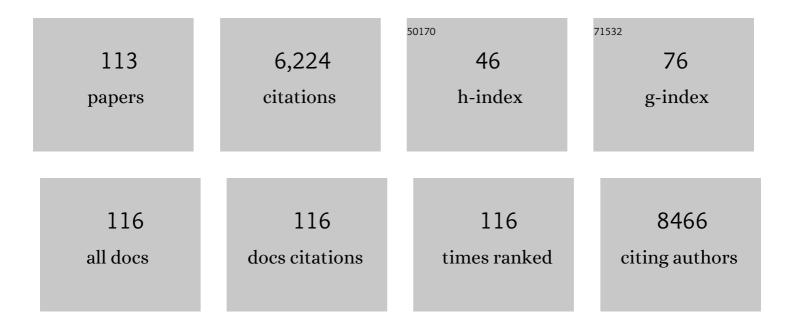
List of Publications by Year in descending order

Source: https://exaly.com/author-pdf/1226877/publications.pdf Version: 2024-02-01



#	Article	IF	CITATIONS
1	Utilizing the Spaceâ€Charge Region of the FeNiâ€LDH/CoP pâ€n Junction to Promote Performance in Oxygen Evolution Electrocatalysis. Angewandte Chemie - International Edition, 2019, 58, 11903-11909.	7.2	329
2	Highly Efficient Ag ₂ O/Bi ₂ O ₂ CO ₃ p-n Heterojunction Photocatalysts with Improved Visible-Light Responsive Activity. ACS Applied Materials & Interfaces, 2014, 6, 11698-11705.	4.0	257
3	Bottom-up synthesis of high surface area mesoporous crystalline silicon and evaluation of its hydrogen evolution performance. Nature Communications, 2014, 5, 3605.	5.8	212
4	Highly active nanostructured CoS2/CoS heterojunction electrocatalysts for aqueous polysulfide/iodide redox flow batteries. Nature Communications, 2019, 10, 3367.	5.8	212
5	Novel Bi2S3/Bi2O2CO3 heterojunction photocatalysts with enhanced visible light responsive activity and wastewater treatment. Journal of Materials Chemistry A, 2014, 2, 4208.	5.2	203
6	Hierarchical Bi2O2CO3 microspheres with improved visible-light-driven photocatalytic activity. CrystEngComm, 2011, 13, 4010.	1.3	179
7	High stability and superior rate capability of three-dimensional hierarchical SnS2 microspheres as anode material in lithium ion batteries. Journal of Power Sources, 2011, 196, 3650-3654.	4.0	175
8	Dual conductive network-enabled graphene/Si–C composite anode with high areal capacity for lithium-ion batteries. Nano Energy, 2014, 6, 211-218.	8.2	155
9	Co3O4 nanorods/graphene nanosheets nanocomposites for lithium ion batteries with improved reversible capacity and cycle stability. Journal of Power Sources, 2012, 202, 230-235.	4.0	153
10	Honeycomb-like metallic nickel selenide nanosheet arrays as binder-free electrodes for high-performance hybrid asymmetric supercapacitors. Journal of Materials Chemistry A, 2017, 5, 22527-22535.	5.2	141
11	3D hierarchical FeSe2 microspheres: Controlled synthesis and applications in dye-sensitized solar cells. Nano Energy, 2015, 15, 205-215.	8.2	140
12	MnFe2O4–graphene nanocomposites with enhanced performances as anode materials for Li-ion batteries. Physical Chemistry Chemical Physics, 2013, 15, 3939.	1.3	119
13	Boron-doped porous Si anode materials with high initial coulombic efficiency and long cycling stability. Journal of Materials Chemistry A, 2018, 6, 3022-3027.	5.2	113
14	Ultrathin FeSe ₂ Nanosheets: Controlled Synthesis and Application as a Heterogeneous Catalyst in Dye‧ensitized Solar Cells. Chemistry - A European Journal, 2015, 21, 4085-4091.	1.7	108
15	Crystallization of a perovskite film for higher performance solar cells by controlling water concentration in methyl ammonium iodide precursor solution. Nanoscale, 2016, 8, 2693-2703.	2.8	100
16	3D-hierarchical SnS ₂ micro/nano-structures: controlled synthesis, formation mechanism and lithium ion storage performances. CrystEngComm, 2012, 14, 1364-1375.	1.3	98
17	3D hierarchical ZnIn2S4: The preparation and photocatalytic properties on water splitting. International Journal of Hydrogen Energy, 2012, 37, 16986-16993.	3.8	96
18	Polydopamine functionalized graphene/NiFe2O4 nanocomposite with improving Li storage performances. Nano Energy, 2014, 6, 51-58.	8.2	94

#	Article	IF	CITATIONS
19	Regeneration of Metal Sulfides in the Delithiation Process: The Key to Cyclic Stability. Advanced Energy Materials, 2016, 6, 1601056.	10.2	93
20	Interfacial Study To Suppress Charge Carrier Recombination for High Efficiency Perovskite Solar Cells. ACS Applied Materials & Interfaces, 2015, 7, 26445-26454.	4.0	90
21	Selfâ€Assembled Heavy Lanthanide Orthovanadate Architecture with Controlled Dimensionality and Morphology. Chemistry - A European Journal, 2009, 15, 1233-1240.	1.7	88
22	Electrospun carbon nanofibers with surface-attached platinum nanoparticles as cost-effective and efficient counter electrode for dye-sensitized solar cells. Nano Energy, 2015, 11, 550-556.	8.2	88
23	Rationally Designed n–n Heterojunction with Highly Efficient Solar Hydrogen Evolution. ChemSusChem, 2015, 8, 1218-1225.	3.6	87
24	3D-hierarchical Cu3SnS4 flowerlike microspheres: controlled synthesis, formation mechanism and photocatalytic activity for H2 evolution from water. Journal of Materials Chemistry A, 2013, 1, 4316.	5.2	85
25	Rose-like I-doped Bi2O2CO3 microspheres with enhanced visible light response: DFT calculation, synthesis and photocatalytic performance. Journal of Hazardous Materials, 2017, 321, 464-472.	6.5	80
26	Nearly monodispersed In(OH) ₃ hierarchical nanospheres and nanocubes: tunable ligand-assisted synthesis and their conversion into hierarchical In ₂ O ₃ for gas sensing. Journal of Materials Chemistry A, 2013, 1, 735-745.	5.2	79
27	3D-hierarchical NiO–graphene nanosheet composites as anodes for lithium ion batteries with improved reversible capacity and cycle stability. RSC Advances, 2012, 2, 3410.	1.7	76
28	Conversion of Cu2O nanocrystals into hollow Cu2â^'xSe nanocages with the preservation of morphologies. Chemical Communications, 2006, , 4548-4550.	2.2	75
29	CoFe2O4-Graphene Nanocomposites Synthesized through An Ultrasonic Method with Enhanced Performances as Anode Materials for Li-ion Batteries. Nano-Micro Letters, 2014, 6, 307-315.	14.4	75
30	Improved rate capability of Si–C composite anodes by boron doping for lithium-ion batteries. Electrochemistry Communications, 2013, 36, 29-32.	2.3	71
31	Well-defined CoSe ₂ @MoSe ₂ hollow heterostructured nanocubes with enhanced dissociation kinetics for overall water splitting. Nanoscale, 2020, 12, 326-335.	2.8	71
32	Synthesis of 3-D Hierarchical Dendrites of Lead Chalcogenides in Large Scale via Microwave-Assistant Method. Crystal Growth and Design, 2007, 7, 425-429.	1.4	70
33	Incorporation of Co into MoS2/graphene nanocomposites: One effective way to enhance the cycling stability of Li/Na storage. Journal of Power Sources, 2018, 373, 103-109.	4.0	67
34	TiO2 coated urchin-like SnO2 microspheres for efficient dye-sensitized solar cells. Nano Research, 2014, 7, 1154-1163.	5.8	66
35	The Role of Mott–Schottky Heterojunctions in Ag–Ag ₈ SnS ₆ as Counter Electrodes in Dye‣ensitized Solar Cells. ChemSusChem, 2015, 8, 817-820.	3.6	64
36	3D Hierarchical Co–Al Layered Double Hydroxides with Long-Term Stabilities and High Rate Performances in Supercapacitors. Nano-Micro Letters, 2017, 9, 21.	14.4	58

#	Article	IF	CITATIONS
37	Silica Wastes to High-Performance Lithium Storage Materials: A Rational Designed Al ₂ O ₃ Coating Assisted Magnesiothermic Process. Small, 2016, 12, 5281-5287.	5.2	57
38	Three dimensional metal oxides–graphene composites and their applications in lithium ion batteries. RSC Advances, 2015, 5, 8814-8834.	1.7	56
39	Atomically thin layered NiFe double hydroxides assembled 3D microspheres with promoted electrochemical performances. Journal of Power Sources, 2016, 325, 675-681.	4.0	56
40	Band gap-tunable (CuIn)xZn2(1â^'x)S2 solid solutions: preparation and efficient photocatalytic hydrogen production from water under visible light without noble metals. Journal of Materials Chemistry, 2012, 22, 23929.	6.7	55
41	High power and stable P-doped yolk-shell structured Si@C anode simultaneously enhancing conductivity and Li+ diffusion kinetics. Nano Research, 2021, 14, 1004-1011.	5.8	55
42	Porous Si@C ball-in-ball hollow spheres for lithium-ion capacitors with improved energy and power densities. Journal of Materials Chemistry A, 2018, 6, 21098-21103.	5.2	52
43	Rational design and fabrication of skeletal Cu 7 S 4 nanocages for efficient counter electrode in quantum dot-sensitized solar cells. Nano Energy, 2015, 12, 186-196.	8.2	51
44	Rice husk-derived hybrid lithium-ion capacitors with ultra-high energy. Journal of Materials Chemistry A, 2017, 5, 24502-24507.	5.2	49
45	A hierarchical CoFeS ₂ /reduced graphene oxide composite for highly efficient counter electrodes in dye-sensitized solar cells. Dalton Transactions, 2017, 46, 9511-9516.	1.6	49
46	Catalystâ€Free Decarboxylation of Carboxylic Acids and Deoxygenation of Alcohols by Electroâ€Induced Radical Formation. Chemistry - A European Journal, 2020, 26, 3226-3230.	1.7	49
47	Glycerol-crosslinked PEDOT:PSS as bifunctional binder for Si anodes: Improved interfacial compatibility and conductivity. Journal of Colloid and Interface Science, 2020, 565, 270-277.	5.0	48
48	Incorporation of plasmonic Au nanostars into photoanodes for high efficiency dye-sensitized solar cells. Journal of Materials Chemistry A, 2016, 4, 545-551.	5.2	47
49	Improving the catalytic performance of Ni 3 S 4 -PtCo heteronanorods via Mott-Schottky effect toward the reduction of iodine couples in dye-sensitized solar cells. Electrochimica Acta, 2017, 241, 89-97.	2.6	47
50	Control of the morphology and composition of yttrium fluoridevia a salt-assisted hydrothermal method. CrystEngComm, 2010, 12, 199-206.	1.3	46
51	Fe ₃ C nanoparticles encapsulated in highly crystalline porous graphite: salt-template synthesis and enhanced electrocatalytic oxygen evolution activity and stability. Chemical Communications, 2018, 54, 3158-3161.	2.2	46
52	One-step construction of multi-doped nanoporous carbon-based nanoarchitecture as an advanced bifunctional oxygen electrode for Zn-Air batteries. Applied Catalysis B: Environmental, 2020, 265, 118594.	10.8	45
53	Formation of NiFe2O4/Expanded Graphite Nanocomposites with Superior Lithium Storage Properties. Nano-Micro Letters, 2017, 9, 34.	14.4	42
54	The role of Mott–Schottky heterojunctions in PtCo–Cu ₂ ZnGeS ₄ as counter electrodes in dye-sensitized solar cells. Chemical Communications, 2015, 51, 8950-8953.	2.2	41

#	Article	IF	CITATIONS
55	N-type hedgehog-like CuBi ₂ O ₄ hierarchical microspheres: room temperature synthesis and their photoelectrochemical properties. CrystEngComm, 2015, 17, 4019-4025.	1.3	39
56	Fe doping promoted electrocatalytic N2 reduction reaction of 2H MoS2. Chinese Chemical Letters, 2020, 31, 2487-2490.	4.8	39
57	Efficient Counter Electrode Manufactured from Ag ₂ S Nanocrystal Ink for Dyeâ€ S ensitized Solar Cells. Chemistry - A European Journal, 2015, 21, 15153-15157.	1.7	36
58	Multi-functional NiS2/FeS2/N-doped carbon nanorods derived from metal-organic frameworks with fast reaction kinetics for high performance overall water splitting and lithium-ion batteries. Journal of Power Sources, 2019, 436, 226857.	4.0	36
59	Synthesis of Ni-doped NiO/RGONS nanocomposites with enhanced rate capabilities as anode materials for Li ion batteries. CrystEngComm, 2013, 15, 6663.	1.3	35
60	Direct growth of SnO2 nanorods on graphene as high capacity anode materials for lithium ion batteries. RSC Advances, 2013, 3, 20573.	1.7	35
61	Efficient Ag ₈ GeS ₆ counter electrode prepared from nanocrystal ink for dye-sensitized solar cells. Journal of Materials Chemistry A, 2015, 3, 20359-20365.	5.2	35
62	Na ₂ Ge ₄ O ₉ nanoparticles encapsulated in 3D carbon networks with long-term stability and superior rate capability in lithium ion batteries. Journal of Materials Chemistry A, 2016, 4, 10552-10557.	5.2	35
63	Homogenously hexagonal prismatic AgBiS ₂ nanocrystals: controlled synthesis and application in quantum dot-sensitized solar cells. CrystEngComm, 2015, 17, 1902-1905.	1.3	34
64	Synergistically Enhanced Electrochemical Performance of Ni3S4–PtX (X = Fe, Ni) Heteronanorods as Heterogeneous Catalysts in Dye-Sensitized Solar Cells. ACS Applied Materials & Interfaces, 2017, 9, 27607-27617.	4.0	32
65	Hierarchical Cu7S4 nanotubes assembled by hexagonal nanoplates with high catalytic performance for quantum dot-sensitized solar cells. Journal of Power Sources, 2015, 299, 212-220.	4.0	31
66	Dye-Sensitized Solar Cells Based on Porous Hollow Tin Oxide Nanofibers. IEEE Transactions on Electron Devices, 2015, 62, 2027-2032.	1.6	29
67	Co stabilized metallic 1Td MoS2 monolayers: Bottom-up synthesis and enhanced capacitance with ultra-long cycling stability. Materials Today Energy, 2018, 7, 10-17.	2.5	28
68	Chemical Coupled PEDOT:PSS/Si Electrode: Suppressed Electrolyte Consumption Enables Long-Term Stability. Nano-Micro Letters, 2021, 13, 54.	14.4	27
69	Activation of Passive Nanofillers in Composite Polymer Electrolyte for Higher Performance Lithiumâ€ion Batteries. Advanced Sustainable Systems, 2017, 1, 1700043.	2.7	26
70	Facile Synthesis of Porous Zn–Sn–O Nanocubes and Their Electrochemical Performances. Nano-Micro Letters, 2016, 8, 174-181.	14.4	25
71	The combination of intercalation and conversion reactions to improve the volumetric capacity of the cathode in Liâ \in "S batteries. Journal of Materials Chemistry A, 2019, 7, 3618-3623.	5.2	25
72	Nanoscale control of grain boundary potential barrier, dopant density and filled trap state density for higher efficiency perovskite solar cells. InformaÄnÄ-Materiály, 2020, 2, 409-423.	8.5	25

#	Article	IF	CITATIONS
73	SnO ₂ /C composites fabricated by a biotemplating method from cotton and their electrochemical performances. CrystEngComm, 2014, 16, 3318-3322.	1.3	24
74	Sandwiched Cu7S4@graphite felt electrode for high performance aqueous polysulfide/iodide redox flow batteries: Enhanced cycling stability and electrocatalytic dynamics of polysulfides. Materials Chemistry and Physics, 2020, 250, 123143.	2.0	24
75	Si@SiOx/Graphene Nanosheets Composite: Ball Milling Synthesis and Enhanced Lithium Storage Performance. Frontiers in Materials, 2018, 4, .	1.2	23
76	Low cost, robust, environmentally friendly, wood supported 3D-hierarchical Cu3SnS4 for efficient solar powered steam generation. Journal of Colloid and Interface Science, 2022, 615, 707-715.	5.0	23
77	A candidate strategy to achieve high initial Coulombic efficiency and long cycle life of Si anode materials: exterior carbon coating on porous Si microparticles. Materials Today Energy, 2017, 5, 299-304.	2.5	22
78	Self-Supported NaTi ₂ (PO ₄) ₃ Nanorod Arrays: Balancing Na ⁺ and Electron Kinetics via Optimized Carbon Coating for High-Power Sodium-Ion Capacitor. ACS Applied Materials & Interfaces, 2020, 12, 50388-50396.	4.0	22
79	Colloidal synthesis of wurtz-stannite Cu ₂ CdGeS ₄ nanocrystals with high catalytic activity toward iodine redox couples in dye-sensitized solar cells. Chemical Communications, 2016, 52, 10866-10869.	2.2	21
80	AgIn _x Ga _{1â^'x} S ₂ solid solution nanocrystals: synthesis, band gap tuning and photocatalytic activity. CrystEngComm, 2014, 16, 10123-10130.	1.3	20
81	Cubeâ€in ube Hollow Cu ₉ S ₅ Nanostructures with Enhanced Photocatalytic Activities in Solar H ₂ Evolution. Chemistry - A European Journal, 2014, 20, 13576-13582.	1.7	19
82	Magnetite modified graphene nanosheets with improved rate performance and cyclic stability for Li ion battery anodes. RSC Advances, 2012, 2, 4397.	1.7	18
83	Hierarchical Cu _{2â^'X} Se nanotubes constructed by two-unit-cell-thick nanosheets: room-temperature synthesis and promoted electrocatalytic activity towards polysulfides. Journal of Materials Chemistry A, 2016, 4, 4790-4796.	5.2	18
84	Cu ₂ CoGeS ₄ nanocrystals for high performance aqueous polysulfide/iodide redox flow batteries: enhanced selectively towards the electrocatalytic conversion of polysulfides. Sustainable Energy and Fuels, 2020, 4, 2892-2899.	2.5	18
85	Copper vacancy activated plasmonic Cu3â°xSnS4 for highly efficient photocatalytic hydrogen generation: Broad solar absorption, efficient charge separation and decreased HER overpotential. Nano Research, 2021, 14, 3358-3364.	5.8	18
86	Utilizing the Spaceâ€Charge Region of the FeNiâ€LDH/CoP pâ€n Junction to Promote Performance in Oxygen Evolution Electrocatalysis. Angewandte Chemie, 2019, 131, 12029-12035.	1.6	17
87	Photogenerated reactive oxygen species and hyperthermia by Cu3SnS4 nanoflakes for advanced photocatalytic and photothermal antibacterial therapy. Journal of Nanobiotechnology, 2022, 20, 195.	4.2	15
88	Bromine and oxygen redox species mediated highly selective electro-epoxidation of styrene. Organic Chemistry Frontiers, 2022, 9, 436-444.	2.3	14
89	Design and synthesis of the composites of multiporous NiMnO 3 micro-nano structure spheres and graphene with alleviated side reaction and enhanced performances as anode materials for lithium ion batteries. Journal of Alloys and Compounds, 2017, 716, 270-277.	2.8	13
90	Asymmetric Activation of the Nitro Group over a Ag/Graphene Heterointerface to Boost Highly Selective Electrocatalytic Reduction of Nitrobenzene. ACS Applied Materials & Interfaces, 2022, 14, 25478-25489.	4.0	13

#	Article	IF	CITATIONS
91	Fe _{1â€x} Co _x S ₂ Solid Solutions with Tunable Energy Structures to Enhance the Performance of Triiodide Reduction in Dyeâ€Sensitized Solar Cells. ChemNanoMat, 2018, 4, 1043-1047.	1.5	12
92	Flower-like SnS ₂ composite with 3D pyrolyzed bacterial cellulose as the anode for lithium-ion batteries with ultralong cycle life and superior rate capability. Dalton Transactions, 2019, 48, 833-838.	1.6	12
93	A Facile Synthesis of Urchin‣ike ZnMn 2 O 4 Architectures with Enhanced Electrochemical Lithium Storage. ChemistrySelect, 2020, 5, 1491-1495.	0.7	12
94	Light absorption, photocarrier dynamic properties of hierarchical SnS2 microspheres and their performances on photodegradation of high concentration Rhodamine B. Journal of Photochemistry and Photobiology A: Chemistry, 2021, 415, 113320.	2.0	11
95	Donorâ~ï€â€"Acceptor Heterosystem-Functionalized Porous Hollow Carbon Microsphere for High-Performance Li–S Cathode Materials with S up to 93 wt %. ACS Applied Materials & Interfaces, 2021, 13, 48872-48880.	4.0	11
96	Controlled synthesis of monodispersed AgGaS2 3D nanoflowers and the shape evolution from nanoflowers to colloids. Journal of Solid State Chemistry, 2011, 184, 1227-1235.	1.4	9
97	The fabrication of hollow cubic-like CuInS2 cages using Cu2O crystals as sacrificing template. Materials Chemistry and Physics, 2013, 143, 15-18.	2.0	9
98	Carbon coated porous silicon flakes with high initial coulombic efficiency and long-term cycling stability for lithium ion batteries. Sustainable Energy and Fuels, 2019, 3, 2361-2365.	2.5	7
99	Photovoltaic Counter Electrodes: An Alternative Approach to Extend Light Absorption Spectra and Enhance Performance of Dyeâ€Sensitized Solar Cells. ChemPlusChem, 2019, 84, 241-246.	1.3	7
100	Bioinspired Activation of <scp>N₂</scp> on Asymmetrical Coordinated Fe Grafted <scp>1T MoS₂</scp> at Room Temperature ^{â€} . Chinese Journal of Chemistry, 2021, 39, 1898-1904.	2.6	7
101	Artificial cathode solid electrolyte interphase to endow highly stable lithium storage of FeF2 nanocrystals. Science China Materials, 2022, 65, 629-636.	3.5	7
102	Flow Electrochemistry Enables Microbial Atmospheric CO ₂ Fixation via Coupling with Iodine-Mediated Organic Reactions. ACS Sustainable Chemistry and Engineering, 2022, 10, 541-551.	3.2	7
103	Porous urchin-like 3D Co(<scp>ii</scp>)Co(<scp>iii</scp>) layered double hydroxides for high performance heterogeneous Fenton degradation. CrystEngComm, 2021, 23, 1234-1242.	1.3	6
104	Rectified SiC-Fe2O3 heterostructures for high efficient activation and degradation of sulfur hexafluoride in air atmosphere. Chemical Engineering Journal, 2022, 450, 137949.	6.6	6
105	Water Soluble CuInSe ₂ Nanoplates: Controlled Synthesis, Photoelectric Response and Electrocatalytic Reduction of Polysulfides. ChemNanoMat, 2015, 1, 52-57.	1.5	5
106	Al ₂ O ₃ coated metal sulfides: one-pot synthesis and enhanced lithium storage stability via localized in situ conversion reactions. Dalton Transactions, 2017, 46, 1260-1265.	1.6	5
107	Morphology genetic 3D hierarchical SnO ₂ microstructures constructed by Sub 5 nm nanocrystals for highly sensitive ethanol-sensor. Nanotechnology, 2021, 32, 485503.	1.3	5
108	Selective Electrosynthesis of 2,5â€Diformylfuran in a Continuousâ€Flow System. ChemSusChem, 2022, 15, .	3.6	5

#	Article	IF	CITATIONS
109	A highly efficient nano-graphite electron transport layer for high performance ZnO/Si solar cells. Sustainable Energy and Fuels, 2018, 2, 820-826.	2.5	3
110	Cubeâ€in ube Hollow Cu ₉ S ₅ Nanostructures with Enhanced Photocatalytic Activities in Solar H ₂ Evolution. Chemistry - A European Journal, 2014, 20, 13413-13413.	1.7	2
111	Interlocked 3D active carbon fibers and monolithic I-doped Bi2O2CO3 structure built by 2D face-to-face interaction: endowed with cycling stability and photocatalytic activity. CrystEngComm, 2021, 23, 3204-3211.	1.3	2
112	A sol-hydrothermal route to truncated tetragonal bipyramid nanocrystals and hierarchical hollow microspheres of anatase TiO2 for application in dye-sensitized solar cells. RSC Advances, 2016, 6, 69798-69806.	1.7	1
113	Metal Oxide Nanocrystals and Their Properties for Application in Solar Cells. , 2014, , 671-707.		1